

# Enhanced Sensitivity in Electrochemical Detection of Ochratoxin A within Food Samples Using Ferrocene- and Aptamer-Tethered Gold Nanoparticles on Disposable Electrodes

Wicem Argoubi,<sup>1</sup> Faisal K. Algethami,<sup>2\*</sup> and Nouredine Raouafi<sup>1\*</sup>

<sup>1</sup> Sensors and Biosensors Group, ACE-Lab (LR99ES15), Faculty of Science, University of Tunis El Manar, 2092 Tunis El Manar, Tunisia.

<sup>2</sup> Department of Chemistry, College of Science, Imam Mohammad Ibn Saud Islamic University (IMSIU), P.O. Box 90950, Riyadh 11623, Saudi Arabia.

Corresponding author:

\*Corresponding author Emails: noureddine.raouafi@fst.utm.tn (Nouredine Raouafi), falgethami@imamu.edu.sa (Faisal K. Algethami).

## ABSTRACT

Ensuring food security is crucial for public health, and the presence of mycotoxins, produced by fungi in improperly stored processed or unprocessed food, poses a significant threat. This research introduces a novel approach –a disposable aptasensing platform designed for the detection of ochratoxin A (OTA). The platform employs gold-nanostructured screen-printed carbon electrodes functionalized with a ferrocene derivative, serving as an integrated faradic transducing system, and an anti-OTA aptamer as a bioreceptor site. Detection relies on the ferrocene electrochemical signal changes induced by the aptamer folding in the presence of the target molecule. Remarkably sensitive, the platform detects OTA within the range of 0.5 to 70 ng·mL<sup>-1</sup> and a detection limit of 11 pg·mL<sup>-1</sup>. This limit is approximately 180 times below the levels stipulated by the European Commission for agricultural commodities. Notably, the sensing device exhibits efficacy in detecting OTA in complex media, such as roasted coffee beans and wine, without the need for sample pretreatment, yielding accurate recoveries. Furthermore, while label-free electrochemical aptasensors have proliferated, this study addresses a gap in understanding the binding mechanisms of some aptasensors. To enhance the experimental findings, a theoretical study was conducted to underscore the specificity of the anti-OTA aptamer as a donor for OTA detection. Molecular docking technique was employed to unveil the key binding region of the aptamer, providing valuable insights into the aptasensor specificity.

## KEYWORDS

Ochratoxin A; Aptasensor; Ferrocene; AuNPs; DPV; Real Samples; Docking.

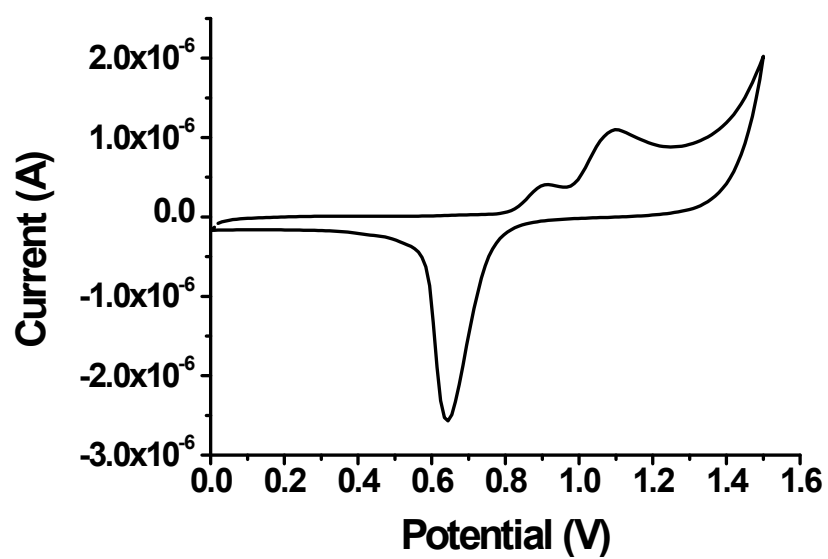


**Figure S1.** CV electrochemical curve oxidation and reduction of modified screen-printed carbon electrode after electrodeposition of gold nanoparticles (20 nm) in a 0.5 M sulfuric acid solution.

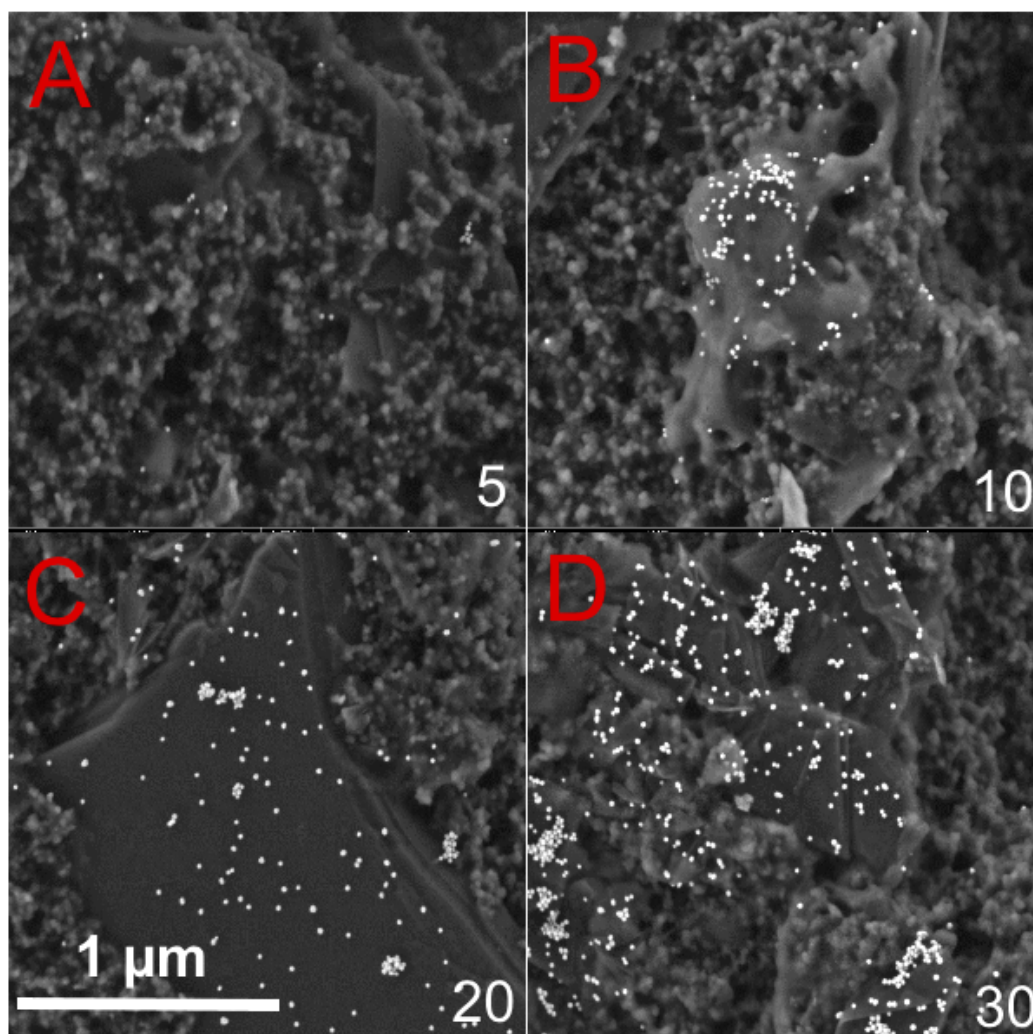


**Figure S2.** SEM images of the modified carbon electrodes obtained after the electrodeposition of gold nanoparticles using: (A) 5 CV cycles, (B) 10 CV cycles, (C) 20 CV cycles and (D) 30 CV cycles.

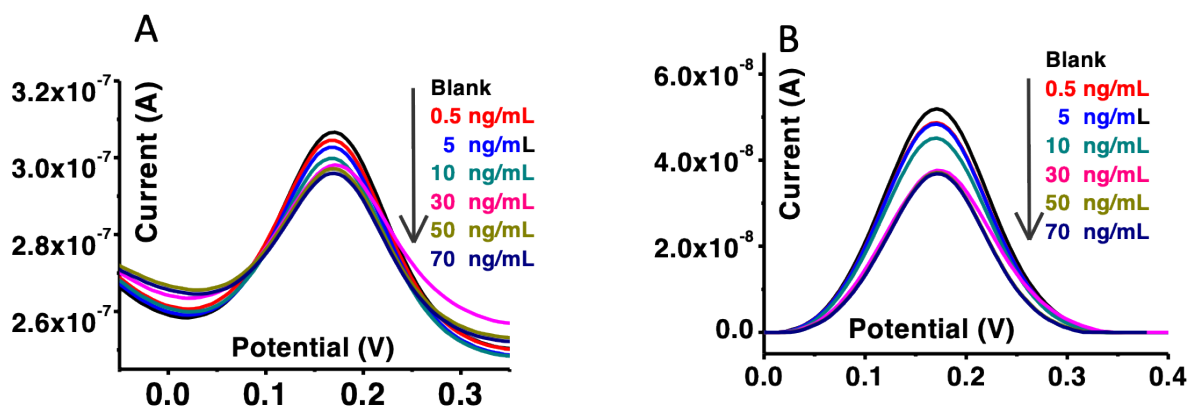


**Figure S3.** (A) uncorrected and (B) baseline-corrected DPV curves of the successive additions of known amounts of OTA to the aptamer-modified AuNPs/SPCE electrode.

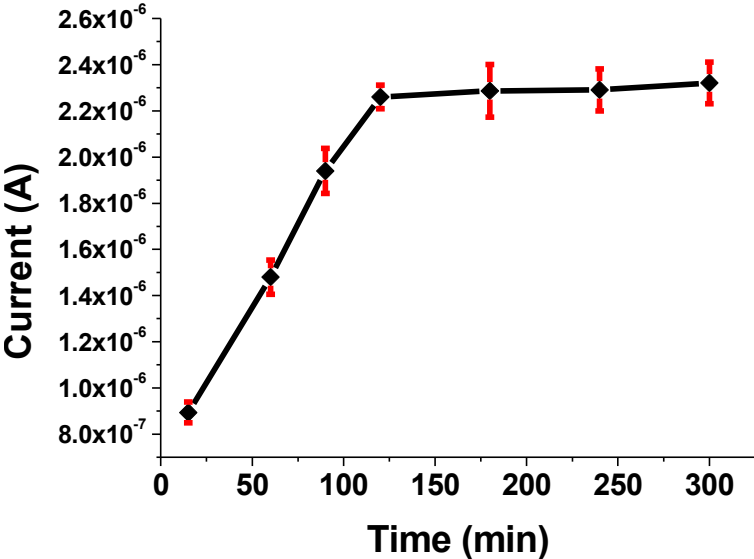


**Figure S4.** Current-concentration response of the electrode for all the tested values of OTA concentration.

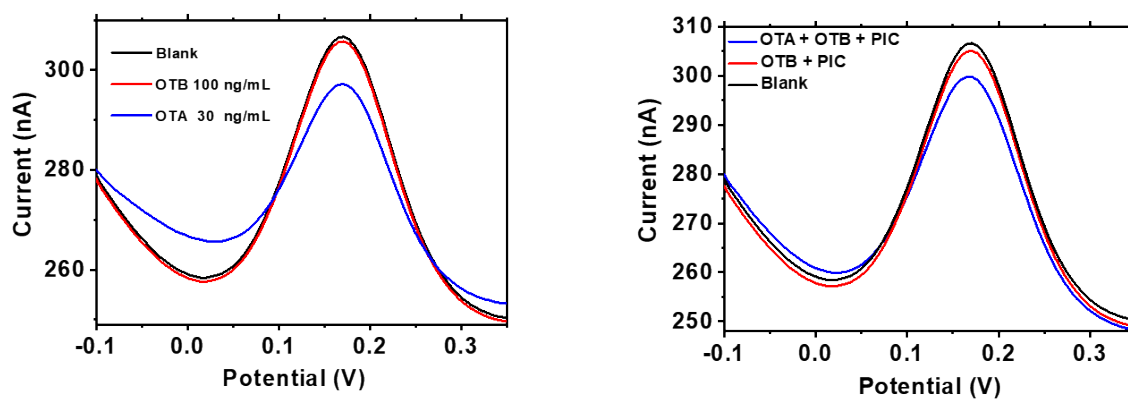


**Figure S5.** DPV curves obtained for the selectivity tests.

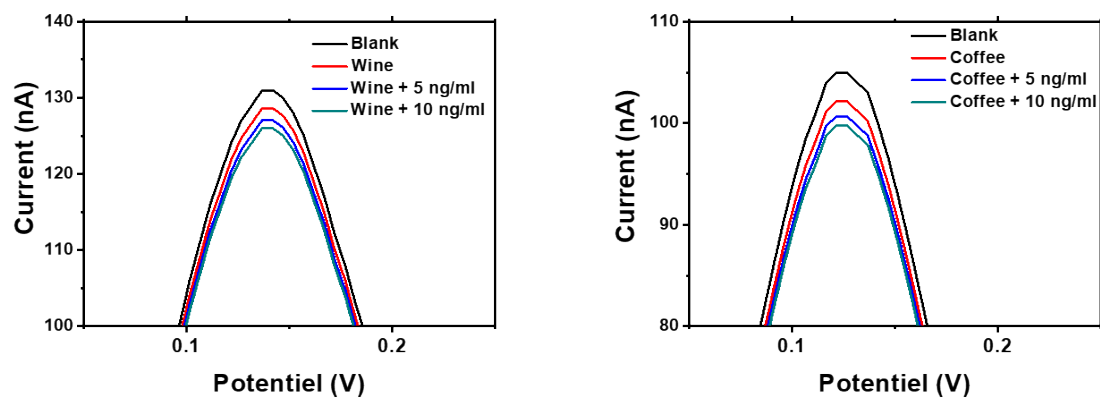


**Figure S6.** Current-concentration response of the electrode for all the tested values of OTA concentration.

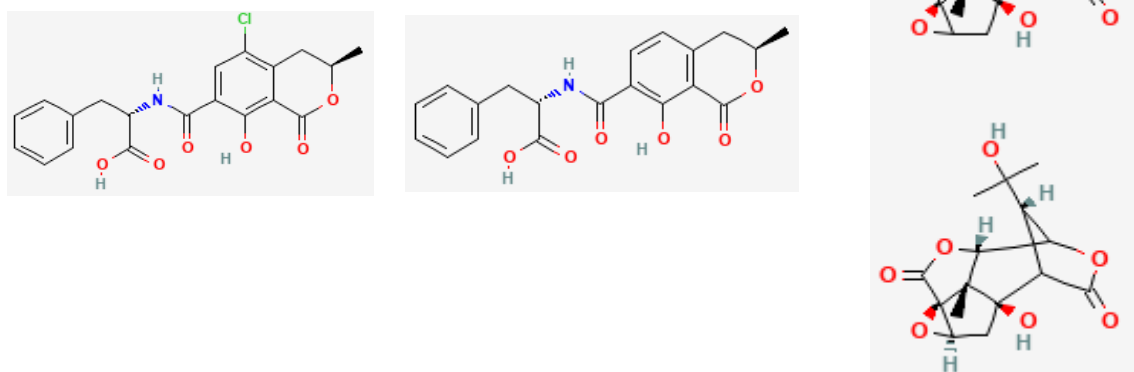


**Figure S7.** Chemicals structure of ochratoxin A (OTA), ochratoxin B (OTB) and picrotoxin (PIC). Detailed information about the three mycotoxins and their properties can be found on PUBCHEM:

OTA: <https://pubchem.ncbi.nlm.nih.gov/compound/442530>

OTB: <https://pubchem.ncbi.nlm.nih.gov/compound/20966>

PIC: <https://pubchem.ncbi.nlm.nih.gov/compound/31304>

**Tableau S1.** Comparative study of the measured current density of the ferrocene versus the

Method modification	Electrodeposition of AuNPs	Drop casting of AuNPs	Electrodeposition AuCl <sub>4</sub> <sup>-</sup>
Calculated charge from gold reduction (μC)	12.91	48.55	66.07
quantity of charge variation (μC)	0.45	0.63	1.05
Current density (J) * 10 <sup>6</sup> (μA/cm <sup>2</sup> )	6.06	1.53	1.04
Density variation * 10 <sup>6</sup> (μA/cm <sup>2</sup> )	0.09	0.03	0.02

amount of charge deposited.

**Table S2.** Results of the molecular docking using AutoDock Vina program

Model	Affinity Kcal/mol	Distance from best model	
		rmsd l.b.	rmsd u.b.
1	-9.0	0.000	0.000
2	-8.2	1.429	2.464
3	-8.0	11.876	15.987
4	-7.9	4.453	7.838
5	-7.8	2.263	3.040
6	-7.7	11.339	14.234
7	-7.6	10.538	14.995
8	-7.6	10.866	15.595
9	-7.5	12.474	16.735

**Table S3.** H-bonds interactions between aptamer and OTA

<b>Contact</b>		<b>Type</b>	<b>Mean</b>	<b>Score (%)</b>
ADE26	OTA	hbond	1.012	101.2
GUA1	OTA	hbond	1.895	189.5
GUA25	OTA	hbond	2.208	220.8
ADE2	OTA	hbond	4.589	458.9
THY3	OTA	hbond	4.675	467.5
ADE34	OTA	hbond	4.926	492.6

**Table S4.** Free energies for the solvated systems and details of the energy contributions.

<b>Complex</b>	<b><math>\Delta G_{(\text{binding,slvd})}</math> (kcal/mol)</b>	<b><math>\Delta E_{\text{vdw}}</math> (kcal/mol)</b>	<b><math>\Delta E_{\text{elec}}</math> (kcal/mol)</b>	<b><math>\Delta G_{\text{pol}}</math> (kcal/mol)</b>	<b><math>\Delta G_{\text{nonpol}}</math> (kcal/mol)</b>
<b>Aptamer/OTA</b>	-9.220	-27.110	-7.330	27.290	-1.720